Densely Nested Top-Down Flows for Salient Object Detection

Chaowei Fang[1†], Haibin Tian[2†], Dingwen Zhang[2∗], Qiang Zhang[2], Jungong Han[3] & Junwei Han[4]

[1]*School of Artificial Intelligence, Xidian University, Xi'an 710071, China;*
[2]*School of Mechano-Electronic Engineering, Xidian University, Xi'an 710071, China;*
[3]*Department of Computer Science, Aberystwyth University, Aberystwyth, Wales;*
[4]*Brain and Artificial Intelligence Laboratory, School of Automation, Northwestern Polytechnical University, Xi'an 710072, China*

Abstract   With the goal of identifying pixel-wise salient object regions from each input image, salient object detection (SOD) has been receiving great attention in recent years. One kind of mainstream SOD methods is formed by a bottom-up feature encoding procedure and a top-down information decoding procedure. While numerous approaches have explored the bottom-up feature extraction for this task, the design on top-down flows still remains under-studied. To this end, this paper revisits the role of top-down modeling in salient object detection and designs a novel densely nested top-down flows (DNTDF)-based framework. In every stage of DNTDF, features from higher levels are read in via the progressive compression shortcut paths (PCSP). The notable characteristics of our proposed method are as follows. 1) The propagation of high-level features which usually have relatively strong semantic information is enhanced in the decoding procedure; 2) With the help of PCSP, the gradient vanishing issues caused by non-linear operations in top-down information flows can be alleviated. 3) Thanks to the full exploration of high-level features, the decoding process of our method is relatively memory efficient compared against those of existing methods. Integrating DNTDF with EfficientNet, we construct a highly light-weighted SOD model, with very low computational complexity. To demonstrate the effectiveness of the proposed model, comprehensive experiments are conducted on six widely-used benchmark datasets. The comparisons to the most state-of-the-art methods as well as the carefully-designed baseline models verify our insights on the top-down flow modeling for SOD. The code of this paper is available at https://github.com/new-stone-object/DNTD.

Keywords   salient object detection, top-down flow, densely nested framework, convolutional networks

1   Introduction

Salient object detection [1] aims at performing the pixel-level identification of the salient object region from an input image. Due to its wide-ranging applications in vision and multimedia community, such as object detection [2], video object segmentation [3], and weakly supervised object mining [4], numerous efforts have been made in recent years to develop effective and efficient deep salient object detection frameworks.

As shown in Figure 1, the existing deep salient object detection models can be divided into three typical frameworks. The first one is the bottom-up encoding flow-based salient object detection framework (see Figure 1 (a)). A bottom-up encoder is used for feature extraction, and then a simple classification head is attached on the top of the encoder for predicting the pixel-wise saliency map. Such methods [5–9] occur in relatively early ages in this research field by designing one or multiple forward network paths to predict the saliency maps. To take advantage of multi-stage feature representations, some recent works [10–14] start to incorporate additional network blocks to further explore the side information residing in the features extracted by multiple stages of the forward pathway. The involvement of the learned side information

---

* Corresponding author (email: zhangdingwen2006yyy@gmail.com)
† Chaowei Fang and Haibin Tian have the same contribution to this work.

(a) Bottom-up encoding flow-based framework

(b) Side information fusion-based framework
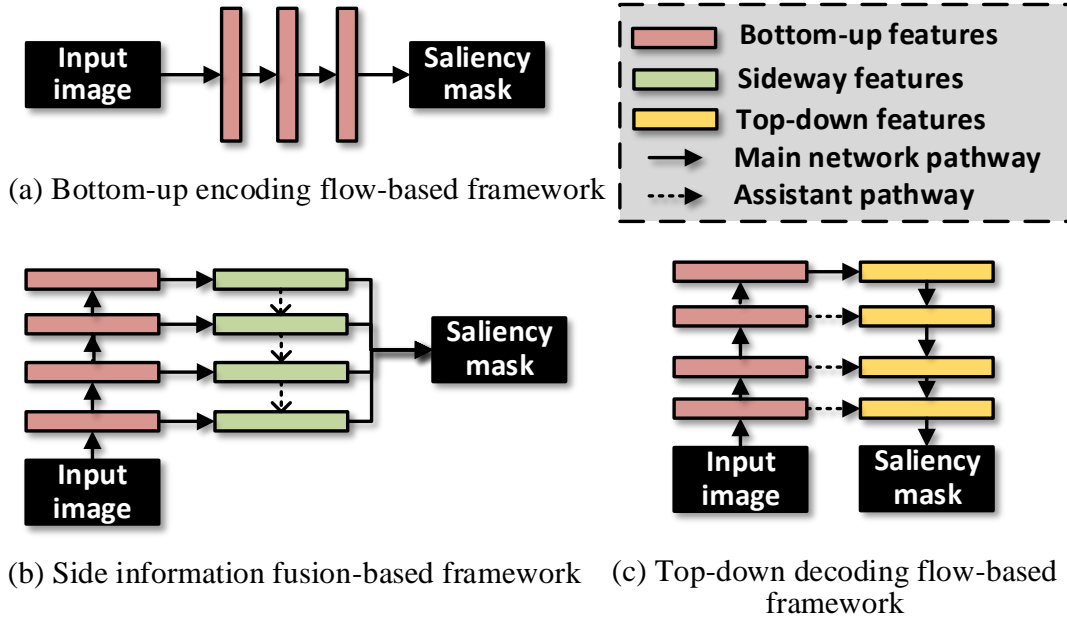
(c) Top-down decoding flow-based framework

Figure 1   A brief illustration of the three mainstream designs of the deep salient object detection frameworks. In (a), the saliency map is derived from the topmost feature map of the backbone. The kind of SOD methods in (b) attempt to explore multi-scale side information. (c) is the most popular decoding framework in SOD, which mines multi-scale features stage by stage.

plays a key role in predicting the desired salient object regions. These works form the second type of learning framework, i.e., the side information fusion-based salient object detection framework (see Figure 1 (b)). Although the side information fusion-based frameworks have achieved great performance gains when compared to the bottom-up encoding flow-based frameworks, one important cue for saliency detection, i.e., the top-down information, has not been adequately explored. To this end, the third type of salient object detection framework occurred, which is named as the top-down decoding flow-based appeared (see Figure 1 (c)). In this framework, the main network pathway is formed by an encoder-decoder architecture, where the decoder explores saliency patterns from the multi-scale semantic embeddings stage by stage and gradually enlarges the resolution of the coarse high-level feature map [15–20]. Notice that this framework may also use the side information to assist the decoding process, but the final saliency masks are obtained from the last decoder stage rather than the fusion stage of the side features.

From the aforementioned top-down decoding flow-based approaches, we observe that their core modeling components still focus on enhancing the side features and merging them into the decoding flow, whereas the top-down information flow remains primitive—propagating from the former decoding stage to the later one as is in the basic encoder-decoder architecture (see Figure 2 (a)). Considering that high-level features possess a great wealth of semantic information, we propose a novel decoding framework, named densely nested top-down flows (see Figure 2 (b)), to enhance the exploration of features extracted from relatively higher levels. In our method, feature maps obtained by each encoding stage are progressively compressed via shortcut paths and propagated to all subsequent decoding stages. The strengthens of our method include the other two strong points. 1) The non-linear operations in the decoding stage are disadvantageous to the gradient back-propagation flow. Hence, the supervision signal propagated from the final prediction to the feature maps of top encoding levels might vanish. For example, if a neuron is not activated by the ReLU function, the gradient flow will be cut off, which means the supervision signal will not be propagated backward. The progressive compression shortcut paths have no non-linear operations, hence they can relieve the gradient vanishing problem. 2) The reuse of high-level features allows a light-weighted decoding network design while achieving high salient object detection performance. Features produced by top layers of the encoder contain relatively strong semantic information which is beneficial to discriminate regions of salient objects from the background. Our method enhances the propagation of these features, resulting to a memory efficient decoding framework.

The overall framework is shown in Figure 3. As can be seen, we use the U-net-like architecture as the main network stream, upon which we further design a novel densely nested top-down flow path to introduce the rich top-down information to the decoding stages. To reduce the computational complexity
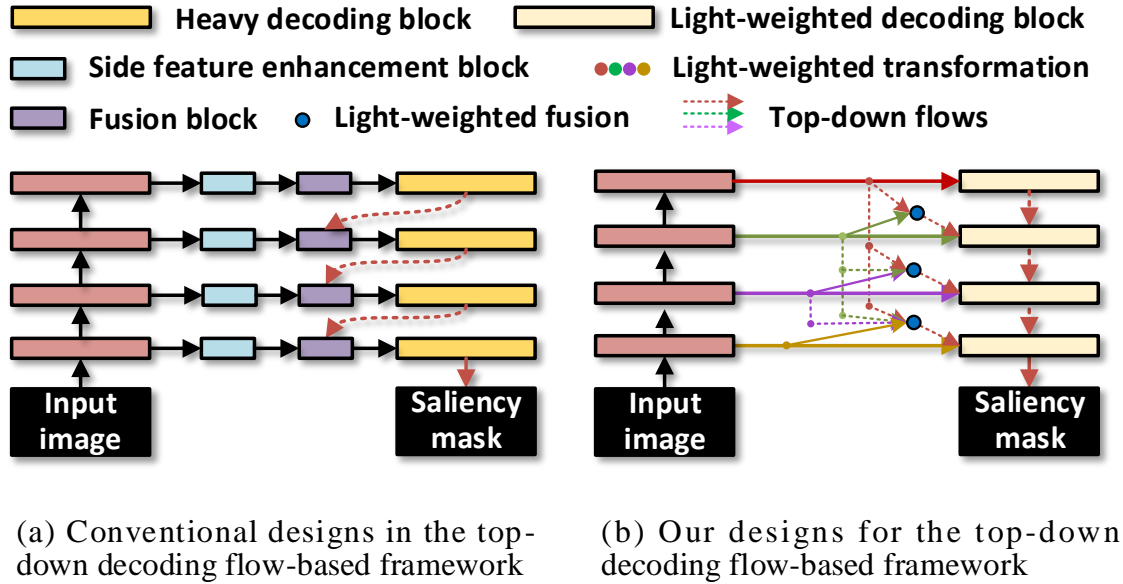
(a) Conventional designs in the top-down decoding flow-based framework

(b) Our designs for the top-down decoding flow-based framework

Figure 2 Comparison between the conventional design and our design for the top-down decoding flow-based salient object detection framework. Our design explores richer semantic information from relatively top stages of the backbone during every decoding stage and complies with the light-weighted principle.

of the decoding stages, we add a 1×1 channel compression layer to each side information pathway. In fact, all the feature pathways in the proposed decoding framework only need to pass through a number of 1×1 convolutional layers together with very small amounts of 3×3 convolutional layers, making the entire network highly lightweight. Meanwhile, the full exploration of top-down information in the proposed DNTD contributes to even better performance than the state-of-the-art SOD methods.

In summary, this work has the following three-fold main contributions: 1) We revisit an important yet under-studied issue, i.e., the top-down flow modeling, of the recent SOD frameworks; 2) We design a highly light-weighted learning framework, via introducing a novel densely nested top-down flow architecture; 3) Comprehensive experiments are conducted, demonstrating the promising detection capacity and the lower computational complexity of the proposed framework. Meanwhile, the insights on top-down modeling are well verified.

2 Related Work

Traditional salient object detection methods are designed based on the hand-crafted features [21–26]. Recently, convolutional neural networks (CNN) have been extensively applied in salient object detection. Thanks to the powerful feature extraction capability of CNN, a great breakthrough has been made in devising effective SOD algorithms. CNN-based SOD frameworks can be categorized into three kinds, including bottom-up encoding flow-based, side information fusion-based, and top-down decoding flow-based framework as shown in Figure 2.

In **bottom-up encoding flow-based framework**, one or multiple forward network pathes are designed to predict the saliency maps. For example, Liu *et al.* [5] propose a multi-resolution convolutional neural network, which has three bottom-up encoding pathways to deal with patches captured from three different resolutions of the input image. A similar idea is also proposed by Li and Yu [6], where a three-pathway framework is devised to extract multi-scale features for every super-pixel and two fully connected layers are adopted to fuse the features and predict the saliency value. In [7], Zhao *et al.* propose a multi-context deep learning framework, which fuses a global-context forward pathway and a local-context forward pathway to obtain the final prediction. In [8], Li *et al.* build a multi-task deep learning model for salient object detection, where a shared bottom-up encoding pathway is used to extract useful deep features and two parallel prediction heads are followed to accomplish the semantic segmentation and saliency estimation, respectively. To learn to refine the saliency prediction results, Wang *et*
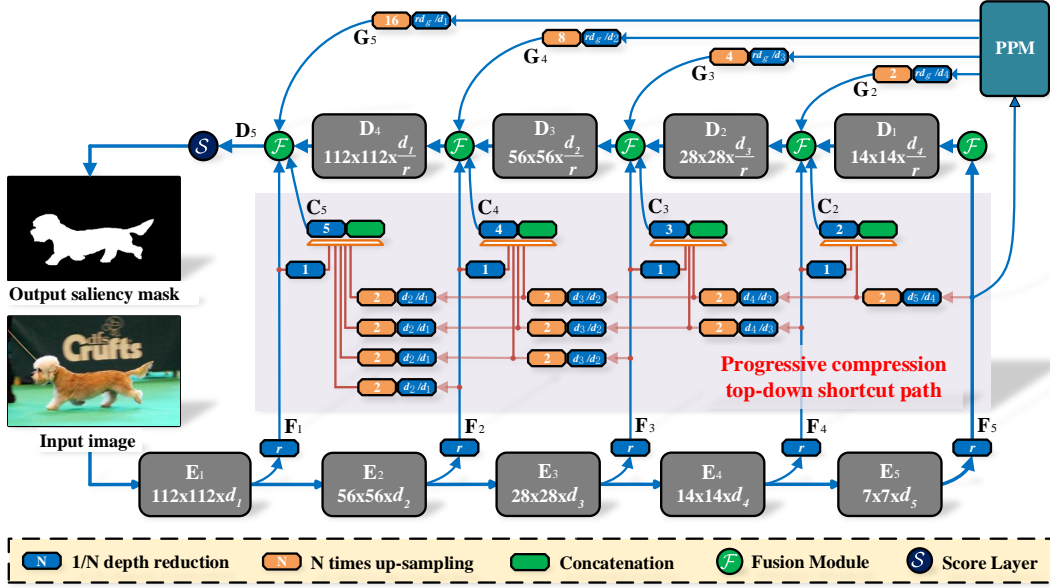
Figure 3 A brief illustration of the proposed salient object detection framework, which is built on a basic U-net-like architecture with the proposed DNTD to complement the rich top-down information into the decoding pathway. Inspired by [19], the PPM is used to involve the global context features. The whole network is built by light-weighted network designs. More details of the network architecture can be referred to in Sec. 3.

al. [9] propose a recurrent fully convolutional network architecture. Specifically, they combine multiple encoding pathways, where saliency prediction results from the former encoding pathway are used to form the input of the latter one.

The **side information fusion-based salient object detection framework** aims to further explore the side information from the features extracted in each stage of the forward pathway. Specifically, based on the network architecture of the holisitcally-nested edge detector [27], Hou *et al.* [10] introduce the skip-layer structures to provide rich multi-scale feature enhancement for exploring the side information. Zhao and Wu [11] propose a simple but effective network architecture. They enhance the low-level and high-level side features in two sperate network streams, where the former is passed through a spatial attention-based stream while the later is passed through a channel attention-based stream. In [12], Wu *et al.* also build a two-stream side information flow. However, different from [11], the two-stream side information flow is designed to fuse the multi-stage features for salient region identification and salient edge detection, respectively. In [13], Su *et al.* use a boundary localization stream and a interior perception stream to explore different side features for obtaining the high-selectivity features and high-invariance features, respectively. Recently, Gao *et al.* [14] propose gOctConv, a flexible convolutional module to efficiently transform and fuse both the intra-stage and cross-stage features for predicting the saliency maps.

To take advantage of top-down information, the third type of salient object detection framework emerges, i.e., the **top-down decoding flow-based framework**. In this framework, the main network pathway is formed by an encoder-decoder architecture, where the decoder recognizes out saliency patterns after fusing multi-scale features progressively. Notice that this framework may also uses the side information to assist the decoding process, but the final saliency masks are obtained from the last decoder stage instead of the fusion stage of the side features. One representative work is proposed by Zhang *et al.* [20], where a U-net [28]-like architecture is used as the basic network and a bi-directional message passing model is introduced into the network to extract rich side features to help each decoding stage. Following this work, Liu *et al.* [19] design a pooling-based U-shape architecture, where they introduce a global guidance module and a feature aggregation module to guide the top-down pathway. In [18], Feng *et al.* propose an Attentive Feedback Module (AFM) and use it to better explore the structure of objects in the side information pathway. Liu *et al.* [17] propose the local attended decoding and global attended decoding schemes for exploring the pixel-wise context-aware attention for each decoding stage.

More recently, in order to better explore the multi-level and multi-scale features, Pang *et al.* [16] design aggregation interaction modules and self-interaction modules and insert them into the side pathway flow and decoding flow, respectively. In [15], Zhao *et al.* propose a gated decoding flow, where multi-level gate units are introduced in the side pathway to transmit informative context patterns to each decoding stage. In this paper, we concentrate on further enhancing the usage of high-level features extracted by the encoder in the decoding flow. A densely nested top-down flows-based decoding framework is proposed to encourage the reuse of high-level features in every stage of the decoding process. Compared to existing top-down decoding flow-based methods, the superiorities of our method are as follows. The gradient vanishing problem caused by the nonlinear operations in the decoding procedure can be mitigated, and a memory efficient decoding network is employed to facilitate the fusion of multi-stage features while maintaining high detection performance.

3   Proposed Method

The purpose of this paper is to settle the saliency object detection problem. Given an RGB image $\mathbf{X}$ with the size of $h \times w$, we propose a novel efficient deep convolutional architecture to predict a saliency map $\mathbf{P} \in [0,1]^{h \times w}$. Every element in $\mathbf{P}$ indicates the saliency probability value of the corresponding pixel. A novel densely nested top-down flow architecture is built up to make full use of high-level feature maps. The semantic information of top layers is propagated to bottom layers through progressive compression shortcut paths. Furthermore, interesting insights are provided to design light-weighted deep convolutional neural networks for salient object detection. Technical details are illustrated in subsequent sections.

3.1   Overview of Network Architecture

The overall network is built upon an encoder-decoder architecture, as shown in Figure 3. After removing the fully connected layers, the backbone of an existing classification model, such as ResNet [29] and EfficientNet [30], is regarded as the encoder. Given an input image $\mathbf{X}$, the encoder is composed of five blocks of convolution layers, which yield 5 feature maps, $\{\mathbf{E}_i\}_{i=1}^{5}$. Every block reduces the horizontal and vertical resolutions into half. Denote the height, width and depth of $\mathbf{E}_i$ be w_i, h_i and d_i, respectively. We have, $h_{i+1} = h_i/2$ and $w_{i+1} = w_i/2$.

The target of the decoder is to infer the pixel-wise saliency map from these feature maps. First of all, a compression unit is employed to reduce the depth of each scale of feature map,

$$\mathbf{F}_i = \mathcal{C}_r(\mathbf{E}_i, \mathbf{W}_i^c), \tag{1}$$

where $\mathcal{C}_r(\cdot, \cdot)$ indicates the calculation procedure of the depth compression unit, consisting of a ReLU layer [31] followed by a 1×1 convolution layer with the kernel of $\mathbf{W}_i^c$. r represents the compression ratio, which means the depth of $\mathbf{F}_i$ is d_i/r. Inspired from [19], the pyramid pooling module (PPM) [32, 33] is used to extract a global context feature map $\mathbf{G}$ (with size of $h_5 \times w_5 \times d_g$) from the last scale of feature map $\mathbf{F}_5$ produced by the encoder. Afterwards, a number of convolution layers are set up to fuse these compressed feature maps $\{\mathbf{F}_i\}_{i=1}^{5}$ and the global feature map $\mathbf{G}$, and output a soft saliency map, based on the U-shape architecture. The distinguishing characteristics of our encoder are reflected in the following aspects: 1) In every stage of the decoder, the features of the top stages of the encoder are accumulated through progressive compression shortcut paths, forming into the feature representation for SOD together with the additional information learned in the current stage. 2) Our decoder is comprised of 1×1 convolutions and a few 3×3 convolutions, which only take up a small number of parameters and consume a small amount of computational cost. The above decoder designs constitute our so-called densely-nested top-down flows.

3.2   Densely Nested Top-Down Flow

In deep convolution neural networks, features extracted by top layers have strong high-level semantic information. These features are advantageous at capturing the discriminative regions of salient objects. Especially, when the network is pretrained on large-scale image recognition datasets, such as Imagenet [34], the top feature maps are intrinsically capable of identifying out salient foreground objects according to [35]. However, their spatial resolutions are usually very coarse which means it is difficult to locate fine object boundaries from them. On the other hand, bottom layers produce responses to local

textural patterns which is beneficial to locate the boundaries of the salient object. Multi-resolution CNN models [5, 6] uses multi-scale copies of the input image to explore both low-level and high-level context information. However, such kind of methods are usually cumbersome and cost heavy computation burden. Inspired by the holistic-nested network architecture [27], fusing multi-scale feature maps produced by different convolution blocks of the encoder is the other popular choice in SOD [10, 36]. U-Net [28], which currently prevails in deep SOD methods [15, 16, 19, 20], accumulates multi-scale feature maps in a more elegant manner. As shown in Figure 1(c), the decoder usually shares the same number of stages with the encoder, and every stage in the decoder merges the feature map of the corresponding stage of the encoder forming a U-shape architecture. However, in a standard U-Net, the features produced by the encoder are fused into the decoder via a simple linear layer. There exists room for improvement in more fully utilizing these features, especially these relatively high-level features. The difficulty for propagating gradients back into the topper layers of the encoder increases as the gradient back propagation process needs to pass through more decoding stages.

For purpose of settling the above issues, we propose a novel top-down flow-based framework, named densely nested top-down flows. Shortcuts are incorporated to feed all feature maps of higher stages into every stage of the decoder. The uniqueness of these shortcuts is that high-level feature maps are progressively compressed and enlarged stage by stage. As shown in Figure 3, $\mathbf{F}_i$ is propagated to the bottom stages successively as follows,

$$\mathbf{F}_{i\to j} = \mathcal{U}p_{\times 2}(\mathcal{C}_{r_j^s}(\mathbf{F}_{i\to j-1}, \mathbf{W}_{i,j}^s)),$$
$$\forall j,\ 5 - i + 2 < j \leqslant 5. \tag{2}$$

Here, $\mathbf{F}_{i\to j}$ indicates the semantic information propagated from $\mathbf{F}_i$ to $\mathbf{F}_j$. $\mathbf{F}_{i\to 5-i+2}(=\mathbf{F}_i)$ is the initial input to the progressive compression shortcut path originated from $\mathbf{F}_i$. $\mathbf{W}_{i,j}^s$ represents weights of a 1×1 convolution kernel, and the compression ratio r_j^s is equal to $\frac{d_{5-j+1}}{d_{5-j+2}}$. $\mathcal{U}p_{\times 2}(\cdot)$ upsamples the height and width of the input feature map into 2 times via the bilinear interpolation. These feature maps $\{\mathbf{F}_i^j\}_{i=5-j+2}^5$ generated by the progressive compression shortcuts are fed into the j-th ($j > 1$) stage of the decoder. No nonlinear function is used in the progressive compression shortcut path. Thus, the shortcut path can facilitate the gradient back-propagation, relieving the gradient vanishing issue caused by the multi-stage decoding process. On the other hand, compared with reducing the depth into the target values at once, our progressive compression mechanism is more efficient, consuming less parameters.

The calculation process in the first stage of the decoder is a transition operation,

$$\mathbf{D}_1 = \mathcal{U}p_{\times 2}(\mathcal{F}(\mathbf{F}_5, \mathbf{W}_1^d)), \tag{3}$$

where $\mathcal{F}(\mathbf{F}_5, \mathbf{W}_1^d)$ consists of a ReLU layer and a 3×3 convolution layer with kernel of $\mathbf{W}$. It transmits $\mathbf{F}_5$ into a $h_4 \times w_4 \times d_4/r$ tensor defined as $\mathbf{D}_1$.

For subsequent stages in the decoder, the calculation process is composed of two fusion steps. First, for the j-th stage of the encoder, we derive an additional feature map from the $(5-j+1)$-th stage of the encoder, $\hat{\mathbf{F}}_{5-j+1} = \mathcal{C}_1(\mathbf{F}_{5-j+1}, \mathbf{W}_{5-j+1}^a)$. The depths of the input and output feature maps are kept the same. Together with $\hat{\mathbf{F}}_{5-j+1}$, the feature maps from higher-level stages are concatenated and compressed into a new context feature map,

$$\mathbf{C}_j = \mathcal{C}_j(\{\hat{\mathbf{F}}_{5-j+1}, \mathbf{F}_{i\to j}|i = 5 - j + 2, \cdots, 5\}, \mathbf{W}_j^f). \tag{4}$$

Note that the above fusion operation compresses the concatenated feature maps with the ratio of j, which indicates the depth of $\mathbf{C}_j$ is d_{5-j+1}/r. The global feature $\mathbf{G}$ is complemented to the j-th stage of the decoder as well, $\mathbf{G}_j = \mathcal{U}p_{\times 2^{j-1}}(\mathcal{C}_{r_j^g}(\mathbf{G}, \mathbf{W}_j^g))$ where $r_j^g = \frac{d_g}{d_{5-j+1}}$. Then, $\mathbf{D}_{j-1}$, $\mathbf{F}_j$, $\mathbf{C}_j$, and $\mathbf{G}_j$ are fused with a pre-placed ReLU and a 3×3 convolution layer, yielding the feature representation of the j-th stage of the decoder,

$$\mathbf{D}_j = \mathcal{U}p_{\times 2}(\mathcal{F}(\{\mathbf{D}_{j-1}, \mathbf{F}_j, \mathbf{C}_j, \mathbf{G}_j\}, \mathbf{W}_j^d)). \tag{5}$$

The depth of $\mathbf{D}_j$ is transformed into d_{5-j}/r. The final output is produced by a score prediction module consisting of a pre-placed ReLU layer, a 1×1 convolution layer and a Sigmoid function $\mathcal{S}(\cdot)$,

$$\mathbf{P} = \mathcal{S}(\mathcal{U}p_{\times 2}(\mathbf{D}_5, \mathbf{W}^o)), \tag{6}$$
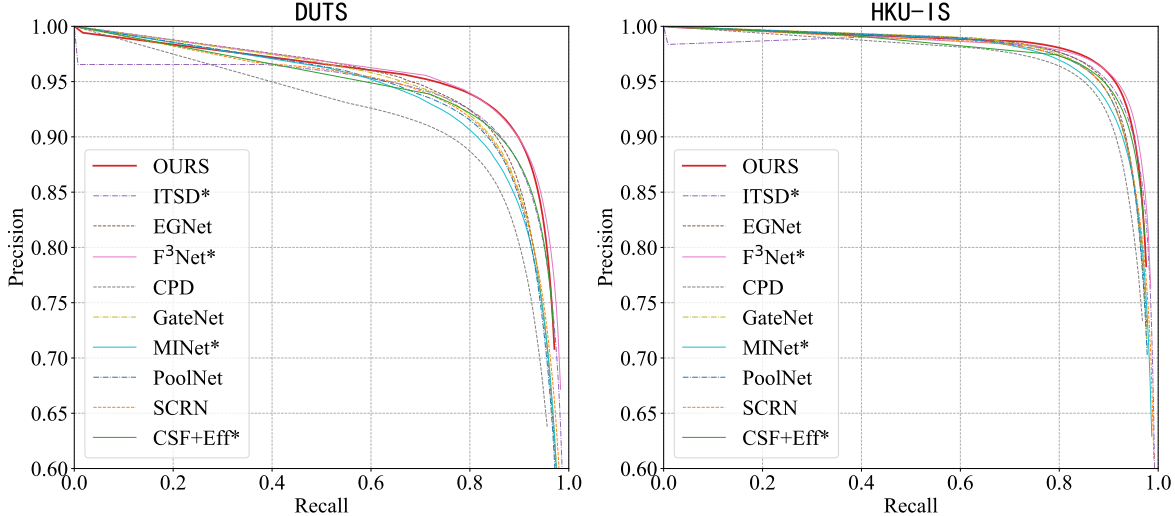
Figure 4 PR curves on the two largest salient object datasets. * denotes the models use the EfficientNet-B3 as the backbone while the rest models use the ResNet50 as the backbone.

where $\mathbf{W}^o$ represents the kernel of the convolution layer, $\mathbf{P}$ ($h \times w \times 1$) is the final predicted saliency map.

The advantage of our densely nested decoder is that every stage is accessible to all higher-level feature maps of the encoder. This framework greatly improves the utilization of high-level features in the top-down information propagation flow.

3.3 Light-Weighted Network Design

In this paper, we are not stacking piles of convolution layers to build a SOD network with high performance. Our devised model has a light-weighted architecture while preserving high performance.

Without backbones initialized with parameters pre-trained on Imagenet, it is difficult to achieve high performance via training a light-weighted backbone from scratch such as CSNet [14]. However, these initialized parameters are learned for solving the image recognition task. This means the features extracted by the pre-trained backbone are responsible for jointly locating the discriminative regions and predicting semantic categories. In the SOD task, it is no longer necessary to recognize the category of the salient object. Considering the above point, we can assume that there exists a large amount of redundant information in the features extracted by the backbone. Hence, in our method, a large value is adopted for the compression ratio r in (1). We empirically find out that using $r \in \{2, 4, 8, 16\}$ has little effects on the SOD performance in our method, as will be illustrated in the experimental section. With the help of a large compression ratio, the computation burden in the decoder can be greatly reduced.

Previous high-performance SOD models are usually equipped with decoders having a moderate amount of calculation complexity. For example, [32] uses multiple 3×3 convolutions to construct a pyramid fusion module in every stage of the decoder. [16] adopts a number of 3×3 convolutions to aggregate inter-level and inter-layer feature maps in the decoder. Cascaded decoders are employed to implement top-down information in [37, 38], which lead to a decoding procedure with large computation burden. In our proposed model, all convolutions adopted in the progressive compression shortcut paths have the kernel size of 1×1. This makes these complicated shortcuts only cost a few weights and computation resources in fact. Furthermore, benefitted from rich top-down information, employing a single 3×3 convolution in every encoder stage is sufficient to construct a high-performance decoder.

The above network designs help us build up an effective and cost-efficient salient object detection model.

Model	Backbone	Param	FLOPs	DUTS-TE			HKU-IS		
				$F_{max}\uparrow$	MAE$\downarrow$	S$\uparrow$	$F_{max}\uparrow$	MAE$\downarrow$	S$\uparrow$
Resnet & VGG									
MLMSNet [39]	VGG16	68.024M	162.515G	0.854	0.048	0.861	0.922	0.039	0.907
BASNet [40]	ResNet34	87.060M	161.238G	0.860	0.047	0.866	0.929	0.032	0.909
CSF+Res2Net [10]	Res2Net	36.529M	13.223G	0.893	0.037	0.890	0.936	0.030	0.921
GateNet [15]	ResNet50	-	-	0.889	0.040	0.885	0.935	0.034	0.915
F³Net [37]	ResNet50	25.537M	10.998G	0.897	0.035	0.888	0.939	0.028	0.917
EGNet [41]	ResNet50	111.660M	198.253G	0.893	0.039	0.885	0.938	0.031	0.918
PoolNet [19]	ResNet50	68.261M	62.406G	0.894	0.036	0.886	0.938	0.030	0.918
MINet [16]	ResNet50	162.378M	70.495G	0.888	0.037	0.884	0.936	0.029	0.919
CPD [42]	ResNet50	47.850M	11.877G	0.865	0.043	0.869	0.925	0.034	0.906
SCRN [12]	ResNet50	25.226M	10.086G	0.888	0.039	0.885	0.934	0.034	0.916
ITSD [38]	ResNet50	26.074M	15.937G	0.883	0.041	0.885	0.934	0.031	0.917
OURS	ResNet50	28.838M	8.083G	0.898	0.033	0.891	0.940	0.028	0.921
More light-weighted backbone									
CSNet [10]	None	0.141M	1.185G	0.819	0.074	0.822	0.899	0.059	0.880
OURS	EfficientNet-B0	4.606M	0.787G	0.891	0.035	0.890	0.936	0.030	0.920
CSF [10]	EfficientNet-B3	12.328M	1.961G	0.892	0.032	0.894	0.936	0.027	0.921
F³Net [37]	EfficientNet-B3	12.588M	5.701G	0.906	0.033	0.898	0.944	0.025	0.926
MINet [16]	EfficientNet-B3	14.793M	7.363G	0.879	0.044	0.875	0.929	0.036	0.909
ITSD [38]	EfficientNet-B3	11.374M	4.148G	0.894	0.041	0.894	0.939	0.034	0.924
OURS	EfficientNet-B3	11.522M	1.738G	0.907	0.030	0.905	0.944	0.027	0.928

Table 1 Quantitative comparison of our method against other SOD methods on DUST-TE and HKU-IS datasets. All these models are trained on DUTS-TR. The performances ranked first, second and third are marked by red, green and blue respectively.

Model	ECSSD			PASCAL-S			DUT-O			SOD		
	$F_{max}\uparrow$	MAE$\downarrow$	S$\uparrow$	$F_{max}\uparrow$	MAE$\downarrow$	S$\uparrow$	$F_{max}\uparrow$	MAE$\downarrow$	S$\uparrow$	$F_{max}\uparrow$	MAE$\downarrow$	S$\uparrow$
CSNet [10]	0.914	0.069	0.888	0.835	0.104	0.813	0.792	0.080	0.803	0.827	0.139	0.747
OURS+EffiB0	0.942	0.038	0.918	0.872	0.063	0.858	0.827	0.052	0.841	0.873	0.099	0.795
CSF [10]	0.944	0.034	0.921	0.872	0.061	0.860	0.826	0.052	0.844	0.881	0.089	0.808
F³Net [37]	0.947	0.032	0.925	0.888	0.058	0.871	0.844	0.056	0.844	0.890	0.083	0.821
MINet [16]	0.936	0.043	0.912	0.873	0.070	0.855	0.813	0.067	0.821	0.858	0.101	0.795
ITSD [38]	0.945	0.042	0.924	0.877	0.065	0.872	0.834	0.058	0.854	0.882	0.096	0.815
OURS	0.950	0.033	0.927	0.888	0.058	0.872	0.844	0.047	0.857	0.893	0.091	0.811

Table 2 Quantitative comparison of our method against other SOD methods on ECSSD, PASCAL-S, DUT-O and SOD datasets. All these models are trained on DUTS-TR. The performances ranked first, second and third are marked by red, green and blue respectively. No pretrained backbone is used in CSNet. 'OURS+EffiB0' indicates the variant of our method using EfficientNet-B0 as the backbone. Other methods use EfficientNet-B3 as the backbone.
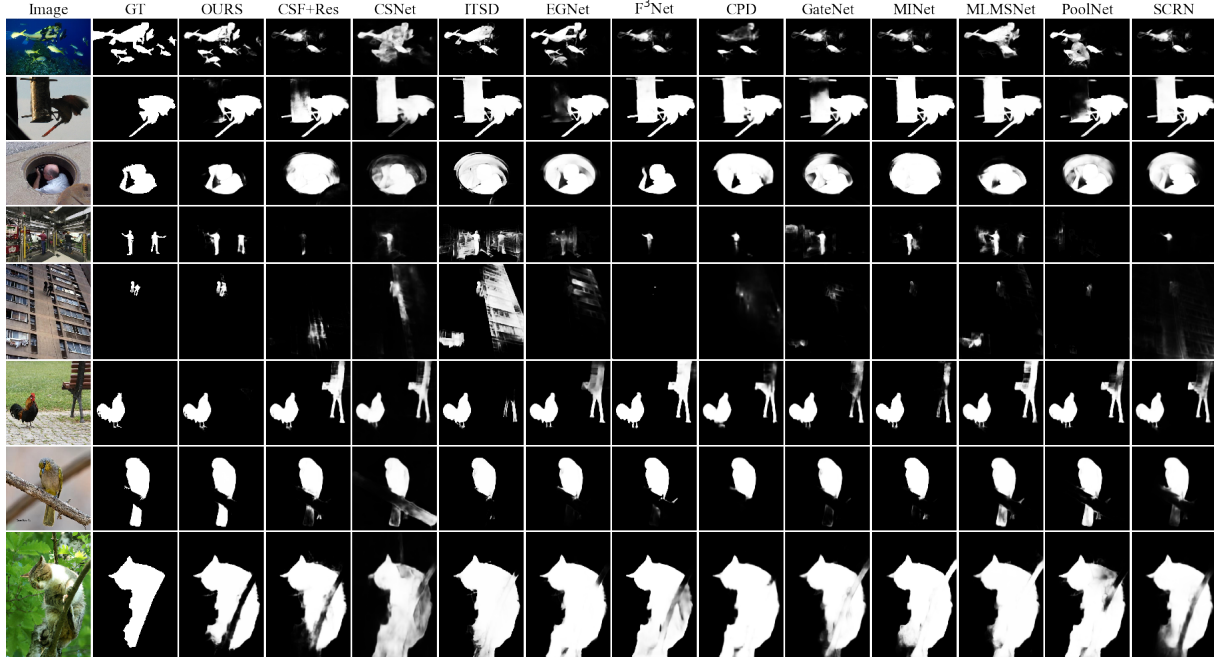
Figure 5   Qualitative comparison of our method against other SOD methods.

3.4   Network Training

To make our model pay more attention to the edge of salient object, we adopt the edge weighted binary cross entropy loss [37] during the training stage,

$$L_{wbce} = \sum_{i=1}^{H} \sum_{j=1}^{W} (1 + \gamma \alpha_{i,j}) BCE(P_{i,j}, Y_{i,j}), \tag{7}$$

$$\alpha_{i,j} = \left| \frac{\sum_{m=-\delta}^{\delta} \sum_{n=-\delta}^{\delta} Y_{i+m,j+n}}{(2\delta + 1)^2} - Y_{ij} \right|, \tag{8}$$

where $BCE(\cdot, \cdot)$ is the binary cross entropy loss function, and γ is a constant. $P_{i,j}$ and $Y_{i,j}$ are the value at position (i, j) of $\mathbf{P}$ and the ground-truth saliency map $\mathbf{Y}$, respectively. $\alpha_{i,j}$ measures the weight assigned to the loss at position (i, j), which receives a relatively large when (i, j) locates around the boundaries of salient objects. δ represents the radius of window size for calculating $\alpha_{i,j}$, and mirrored padding is adopted to fill positions outside the border of the image. Adam [43] is used to optimize network parameters.

4   Experiments

4.1   Datasets & Evaluation Metrics

The DUTS [44] is the largest dataset for salient object detection, containing 10,553 training images (DUTS-TR) and 5,019 testing images (DUTS-TE). Our proposed model is trained with images of DUTS-TR and evaluated on six commonly used salient object detection datasets, including DUTS-TE, HKU-IS [6], ECSSD [45], PASCAL-S [46], DUT-OMRON [21], and SOD [47].

Three metrics are adopted to evaluate the performance of SOD methods, including the maximum of F-measure (F_{max}) [48], mean absolute error (MAE), and S-measure (S) [49].

4.2   Implementation Details

In our experiments, our proposed top-down flow mechanism is integrated with two kinds of backbone models, including ResNet50 [29] and EfficientNet [30]. For ResNet50, we adopt the knowledge distillation
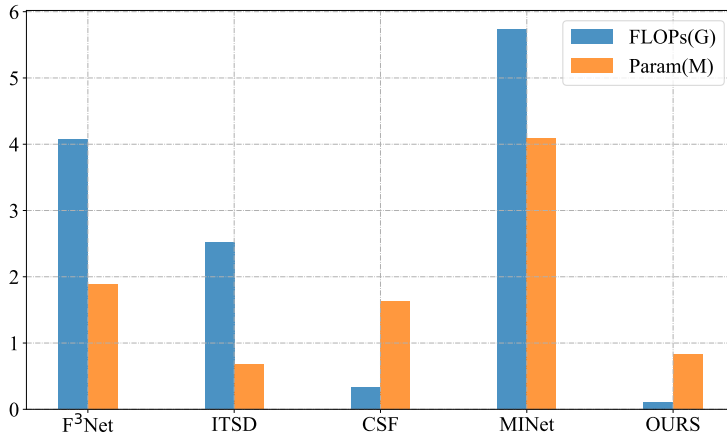
Figure 6 Comparisons of the parameters and FLOPs between different decoders based on EfficientNet-B3.

PCSP	PPM	$\mathbf{F_{max}}$	MAE	S
✗	✗	0.887	0.039	0.883
✗	✓	0.891	0.037	0.886
1	✓	0.891	0.034	0.890
2	✓	0.894	0.034	0.892
3	✓	0.896	0.034	0.891
4	✗	0.891	0.037	0.886
4	✓	**0.898**	**0.033**	**0.891**

Table 3 Ablation study on DUTS-TE dataset, using backbone ResNet50. ✓/✗indicates whether the module is used or not. The number of PCSP denotes the number of most top feature maps of the encoder which are propagated to bottom convolutional blocks of the decoder.

strategy in [50] to initialize network parameters. The other models, EfficientNet-B0 and EfficientNet-B3, are pretrained on Imagenet [51]. The trainable parameters of the decoder are initialized as in [52]. Random horizontal flipping and multi-scale training strategy (0.8,0.9,1.0,1.1 and 1.2 times geometric scaling) are applied for data augmentation. All models are trained with 210 epochs and the batch size is set as 1. The learning rate is initially set to 1.0×10^{-5} and 4.5×10^{-4} respectively for ResNet50 and EfficientNet, and divided by 10 at the at the 168-th epoch. Hyper-parameters in (7) are set as $\gamma = 3$ and $\delta = 10$. A variety of values $\{2, 4, 8, 16, 32\}$ are tested for the compression ratio r. Without specification, r is set as 4, 2 and 2 for ResNet50, EfficientNet-B0 and EfficientNet-B3, respectively. Our proposed model is implemented with PyTorch, and one 11GB NVIDIA GTX 1080Ti GPU is used to train all models.

4.3   Comparison with State-of-the-arts

As presented in Table 1 and 2, we compare our method against various existing SOD methods. For a fair comparison, we reimplemented very recently proposed SOD algorithms, including CSF [14], F^{3}Net [37], MINet [16] and ITSD [38], via replacing their original backbones with EfficientNet-B3. FLOPs are calculated with a 288×288 input image. Table 1 presents experimental results of various SOD methods which use VGG [34], ResNet, and EfficientNet as backbones, on the two largest datasets, DUTS and HKU-IS. Our method surpasses state-of-the-art methods while consuming much fewer FLOPs. When using ResNet50 as backbone, our method achieves marginally better performance than the second best method F^{3}Net [37], and the FLOPs consumed by our method are 2.915G fewer. When integrated with EfficientNet-B3, on the DUTS-TE dataset, the S-measure produced by our method is 0.007 higher than that produced by F^{3}Net, while the FLOPs consumed by our method are 30.48% of those consumed by F^{3}Net. Table 2 showcases SOD performance on the other 4 datasets, including ECSSD, PASCAL-S, DUT-O, and SOD. On the DUT-O dataset, our method gives rise to results having 9.62% lower MAE, compared to the results of CSF. Without using a pre-trained backbone, the performance of CSNet is

DCB	F_{max}	MAE	S	FLOPs	Param
3×3	0.907	0.0305	0.905	0.108G	0.825M
FAM	0.904	0.0312	0.902	0.123G	1.906M

Table 4 Inner comparisons of different variants of our method based on EfficientNet-B3. 'DCB' indicates the convolutional block adopted in every stage of the decoder. 'FAM' means the module containing a single 3×3 convolution operation is replaced with the FAM [19] in every stage of the decoder.

scale	F_{max}	MAE	S	Param	FLOPs
32	0.884	0.036	0.880	379.50K	63.77M
16	0.890	0.035	0.888	840.92K	154.83M
8	0.893	0.034	0.887	2.01M	420.96M
4	0.898	0.033	0.891	5.33M	1.29G
2	0.901	0.031	0.895	15.90M	4.37G

Table 5 Comparisons of performance, parameters and FLOPs which is based on ResNet50 using different compression scale. **Param** and **FLOPs** denote the parameters and FLOPs of the decoder.

inferior though it costs a small number of parameters and FLOPs. On the basis of EfficientNet-B0, our proposed method contributes to a very efficient SOD model which has less FLOPs than CSNet while maintaining appealing SOD performance. Overall, our method achieves the best performance across backbone models.

In addition, We follow [41] to compare the precision-recall curves of our approach with the state-of-the-art methods on the DUTS and HKU-IS datasets. A gallery of SOD examples is also visualized in Figure 5 for qualitative comparisons. Our method performs clearly better than other methods, across small and large salient objects.

4.4 Ablation Study

Efficacy of Main Components In this experiment, we first verify the efficacy of main components in our proposed model, including the progressive compression shortcut path (PCSP) and the PPM for global feature extraction. ResNet50 is used to construct the backbone of our proposed model and SOD performance is evaluated on the DUTS-TE dataset. The experimental results are presented in Table 3. As more top-down feature maps are used to complement high-level semantic information in bottom convolution layers via multiple PCSPs, the performance of our method increases consistently. The adoption of 4 PCSPs, induces to performance gains of 0.005 (when PPM is not used) and 0.011 (when PPM is used) on the F_{max} metric. Besides, we can observe that the global information provided by the PPM and high-level semantic information provided by the PCSP can complement each other. Without using any of the two modules, performance degradation is caused.

Different Variants of Our Method We further provide inner comparisons between variants of our proposed model, in Table 4. To validate whether more complicated convolution blocks is effective in the decoder of our method, we replace the 3×3 convolution layer with the FAM block used in [19] to build the fusion module of each decoding stage. However, no obvious performance gain is obtained.

4.5 Efficiency Discussions

Analysis of Compression Ratio The influence of using different ratios to compress the features of the encoder as in (1) is illustrated in Table 5. As discussed in Section 3.3, there are large amounts of redundant information in the features extracted by the backbone since it is pre-trained for image recognition. Hence, using a moderately large ratio (up to 16) to compress features of the network backbone has no significant effect on the SOD performance, according to the results reported in Table 5. The benefit of using a large compression ratio is achieving the goal of light-weighted network design in our method while not causing unbearable performance decrease.

Complexity of Decoder As shown in Figure 6, the decoder of our proposed model costs significantly fewer FLOPs than the decoders of recent SOD models, including F^{3}Net, ITSD, CSF and MINet. The parameters and FLOPs are counted using the backbone of Efficient-B3. As can be observed from Table

1 and 2, our method outperforms these methods on most datasets and metrics. This indicates that our method achieves better performance even if less memory is consumed.

5 Conclusion

In this paper, we first revisit existing CNN-based top-down flow architectures. Then, to make full usage of multi-scale high-level feature maps, progressive compression shortcut paths are devised to enhance the propagation semantic information residing in higher-level features of the encoder to bottom convolutional blocks of the decoder, which form the novel densely nested top-down flows. Extensive experiments on six widely-used benchmark datasets indicate that the proposed SOD model can achieve state-of-the-art performance. Notably, the computational complexity and model size of the proposed framework are also very light-weighted.

References

1 Junwei Han, Dingwen Zhang, Gong Cheng, Nian Liu, and Dong Xu. Advanced deep-learning techniques for salient and category-specific object detection: a survey. *IEEE Signal Processing Magazine*, 35(1):84–100, 2018.

2 Tsung-Yi Lin, Piotr Dollár, Ross Girshick, Kaiming He, Bharath Hariharan, and Serge Belongie. Feature pyramid networks for object detection. In *Proceedings of the IEEE conference on computer vision and pattern recognition*, pages 2117–2125, 2017.

3 Dingwen Zhang, Junwei Han, Le Yang, and Dong Xu. Spftn: a joint learning framework for localizing and segmenting objects in weakly labeled videos. *IEEE Transactions on Pattern Analysis and Machine Intelligence*, 2018.

4 Dingwen Zhang, Junwei Han, Long Zhao, and Deyu Meng. Leveraging prior-knowledge for weakly supervised object detection under a collaborative self-paced curriculum learning framework. *International Journal of Computer Vision*, 127(4):363–380, 2019.

5 Nian Liu, Junwei Han, Dingwen Zhang, Shifeng Wen, and Tianming Liu. Predicting eye fixations using convolutional neural networks. In *Proceedings of the IEEE Conference on Computer Vision and Pattern Recognition*, pages 362–370, 2015.

6 Guanbin Li and Yizhou Yu. Visual saliency based on multiscale deep features. In *Proceedings of the IEEE conference on computer vision and pattern recognition*, pages 5455–5463, 2015.

7 Rui Zhao, Wanli Ouyang, Hongsheng Li, and Xiaogang Wang. Saliency detection by multi-context deep learning. In *Proceedings of the IEEE conference on computer vision and pattern recognition*, pages 1265–1274, 2015.

8 Xi Li, Liming Zhao, Lina Wei, Ming-Hsuan Yang, Fei Wu, Yueting Zhuang, Haibin Ling, and Jingdong Wang. Deepsaliency: Multi-task deep neural network model for salient object detection. *IEEE transactions on image processing*, 25(8):3919–3930, 2016.

9 Linzhao Wang, Lijun Wang, Huchuan Lu, Pingping Zhang, and Xiang Ruan. Saliency detection with recurrent fully convolutional networks. In *European conference on computer vision*, pages 825–841. Springer, 2016.

10 Qibin Hou, Ming-Ming Cheng, Xiaowei Hu, Ali Borji, Zhuowen Tu, and Philip HS Torr. Deeply supervised salient object detection with short connections. In *Proceedings of the IEEE Conference on Computer Vision and Pattern Recognition*, pages 3203–3212, 2017.

11 Ting Zhao and Xiangqian Wu. Pyramid feature attention network for saliency detection. In *IEEE Conference on Computer Vision and Pattern Recognition (CVPR)*, 2019.

12 Zhe Wu, Li Su, and Qingming Huang. Stacked cross refinement network for edge-aware salient object detection. In *Proceedings of the IEEE International Conference on Computer Vision*, pages 7264–7273, 2019.

13 Jinming Su, Jia Li, Yu Zhang, Changqun Xia, and Yonghong Tian. Selectivity or invariance: Boundary-aware salient object detection. In *Proceedings of the IEEE International Conference on Computer Vision*, pages 3799–3808, 2019.

14 Shang-Hua Gao, Yong-Qiang Tan, Ming-Ming Cheng, Chengze Lu, Yunpeng Chen, and Shuicheng Yan. Highly efficient salient object detection with 100k parameters. *European conference on computer vision*, 2020.

15 Xiaoqi Zhao, Youwei Pang, Lihe Zhang, Huchuan Lu, and Lei Zhang. Suppress and balance: A simple gated network for salient object detection. In *Eur. Conf. Comput. Vis.*, 2020.

16 Youwei Pang, Xiaoqi Zhao, Lihe Zhang, and Huchuan Lu. Multi-scale interactive network for salient object detection. In *IEEE Conf. Comput. Vis. Pattern Recog.*, June 2020.

17 Nian Liu, Junwei Han, and Ming-Hsuan Yang. Picanet: Learning pixel-wise contextual attention for saliency detection. In *Proceedings of the IEEE Conference on Computer Vision and Pattern Recognition*, pages 3089–3098, 2018.

18 Mengyang Feng, Huchuan Lu, and Errui Ding. Attentive feedback network for boundary-aware salient object detection. In *Proceedings of the IEEE/CVF Conference on Computer Vision and Pattern Recognition (CVPR)*, June 2019.

19 Jiang-Jiang Liu, Qibin Hou, Ming-Ming Cheng, Jiashi Feng, and Jianmin Jiang. A simple pooling-based design for real-time salient object detection. In *IEEE Conference on Computer Vision and Pattern Recognition (CVPR)*, 2019.

20 Lu Zhang, Ju Dai, Huchuan Lu, You He, and Gang Wang. A bi-directional message passing model for salient object detection. In *Proceedings of the IEEE Conference on Computer Vision and Pattern Recognition*, pages 1741–1750, 2018.

21 Chuan Yang, Lihe Zhang, Huchuan Lu, Xiang Ruan, and Ming-Hsuan Yang. Saliency detection via graph-based manifold ranking. In *Proceedings of the IEEE conference on computer vision and pattern recognition*, pages 3166–3173, 2013.

22 Jianming Zhang, Stan Sclaroff, Zhe Lin, Xiaohui Shen, Brian Price, and Radomir Mech. Minimum barrier salient object detection at 80 fps. In *Proceedings of the IEEE international conference on computer vision*, pages 1404–1412, 2015.

23 Ming-Ming Cheng, Niloy J Mitra, Xiaolei Huang, Philip HS Torr, and Shi-Min Hu. Global contrast based salient region detection. *IEEE transactions on pattern analysis and machine intelligence*, 37(3):569–582, 2014.

24 Wangjiang Zhu, Shuang Liang, Yichen Wei, and Jian Sun. Saliency optimization from robust background detection. In *Proceedings of the IEEE conference on computer vision and pattern recognition*, pages 2814–2821, 2014.

25 Huaizu Jiang, Jingdong Wang, Zejian Yuan, Yang Wu, Nanning Zheng, and Shipeng Li. Salient object detection: A discriminative regional feature integration approach. In *Proceedings of the IEEE conference on computer vision and pattern recognition*, pages 2083–2090, 2013.

26   Dominik A Klein and Simone Frintrop. Center-surround divergence of feature statistics for salient object detection. In *2011 International Conference on Computer Vision*, pages 2214–2219. IEEE, 2011.

27   Saining Xie and Zhuowen Tu. Holistically-nested edge detection. In *Proceedings of the IEEE international conference on computer vision*, pages 1395–1403, 2015.

28   Olaf Ronneberger, Philipp Fischer, and Thomas Brox. U-net: Convolutional networks for biomedical image segmentation. In *International Conference on Medical image computing and computer-assisted intervention*, pages 234–241. Springer, 2015.

29   Kaiming He, Xiangyu Zhang, Shaoqing Ren, and Jian Sun. Deep residual learning for image recognition. In *Proceedings of the IEEE conference on computer vision and pattern recognition*, pages 770–778, 2016.

30   Mingxing Tan and Quoc V Le. Efficientnet: Rethinking model scaling for convolutional neural networks. *arXiv preprint arXiv:1905.11946*, 2019.

31   Xavier Glorot, Antoine Bordes, and Yoshua Bengio. Deep sparse rectifier neural networks. In *Proceedings of the fourteenth international conference on artificial intelligence and statistics*, pages 315–323, 2011.

32   Kaiming He, Xiangyu Zhang, Shaoqing Ren, and Jian Sun. Spatial pyramid pooling in deep convolutional networks for visual recognition. *IEEE transactions on pattern analysis and machine intelligence*, 37(9):1904–1916, 2015.

33   Hengshuang Zhao, Jianping Shi, Xiaojuan Qi, Xiaogang Wang, and Jiaya Jia. Pyramid scene parsing network. In *Proceedings of the IEEE conference on computer vision and pattern recognition*, pages 2881–2890, 2017.

34   Olga Russakovsky, Jia Deng, Hao Su, Jonathan Krause, Sanjeev Satheesh, Sean Ma, Zhiheng Huang, Andrej Karpathy, Aditya Khosla, Michael Bernstein, et al. Imagenet large scale visual recognition challenge. *International journal of computer vision*, 115(3):211–252, 2015.

35   Bolei Zhou, Aditya Khosla, Agata Lapedriza, Aude Oliva, and Antonio Torralba. Learning deep features for discriminative localization. In *Proceedings of the IEEE conference on computer vision and pattern recognition*, pages 2921–2929, 2016.

36   G. Li and Y. Yu. Deep contrast learning for salient object detection. In *IEEE Conference on Computer Vision and Pattern Recognition (CVPR)*, pages 478–487, June 2016.

37   Jun Wei, Shuhui Wang, and Qingming Huang. F3net: Fusion, feedback and focus for salient object detection. In *AAAI Conference on Artificial Intelligence (AAAI)*, 2020.

38   Huajun Zhou, Xiaohua Xie, Jian-Huang Lai, Zixuan Chen, and Lingxiao Yang. Interactive two-stream decoder for accurate and fast saliency detection. In *Proceedings of the IEEE/CVF Conference on Computer Vision and Pattern Recognition*, pages 9141–9150, 2020.

39   Runmin Wu, Mengyang Feng, Wenlong Guan, Dong Wang, Huchuan Lu, and Errui Ding. A mutual learning method for salient object detection with intertwined multi-supervision. In *Proceedings of the IEEE Conference on Computer Vision and Pattern Recognition*, pages 8150–8159, 2019.

40   Xuebin Qin, Zichen Zhang, Chenyang Huang, Chao Gao, Masood Dehghan, and Martin Jagersand. Basnet: Boundary-aware salient object detection. In *The IEEE Conference on Computer Vision and Pattern Recognition (CVPR)*, June 2019.

41   Jia-Xing Zhao, Jiang-Jiang Liu, Deng-Ping Fan, Yang Cao, Jufeng Yang, and Ming-Ming Cheng. Egnet:edge guidance network for salient object detection. In *The IEEE International Conference on Computer Vision (ICCV)*, Oct 2019.

42   Zhe Wu, Li Su, and Qingming Huang. Cascaded partial decoder for fast and accurate salient object detection. In *The IEEE Conference on Computer Vision and Pattern Recognition (CVPR)*, June 2019.

43   Diederik P Kingma and Jimmy Ba. Adam: A method for stochastic optimization. *arXiv preprint arXiv:1412.6980*, 2014.

44   Lijun Wang, Huchuan Lu, Yifan Wang, Mengyang Feng, Dong Wang, Baocai Yin, and Xiang Ruan. Learning to detect salient objects with image-level supervision. In *Proceedings of the IEEE Conference on Computer Vision and Pattern Recognition (CVPR)*, July 2017.

45   Qiong Yan, Li Xu, Jianping Shi, and Jiaya Jia. Hierarchical saliency detection. In *Proceedings of the IEEE conference on computer vision and pattern recognition*, pages 1155–1162, 2013.

46   Yin Li, Xiaodi Hou, Christof Koch, James M Rehg, and Alan L Yuille. The secrets of salient object segmentation. In *Proceedings of the IEEE Conference on Computer Vision and Pattern Recognition*, pages 280–287, 2014.

47   Vida Movahedi and James H Elder. Design and perceptual validation of performance measures for salient object segmentation. In *2010 IEEE Computer Society Conference on Computer Vision and Pattern Recognition-Workshops*, pages 49–56. IEEE, 2010.

48   Radhakrishna Achanta, Sheila Hemami, Francisco Estrada, and Sabine Susstrunk. Frequency-tuned salient region detection. In *2009 IEEE conference on computer vision and pattern recognition*, pages 1597–1604. IEEE, 2009.

49   Deng-Ping Fan, Ming-Ming Cheng, Yun Liu, Tao Li, and Ali Borji. Structure-measure: A new way to evaluate foreground maps. In *IEEE International Conference on Computer Vision*, 2017.

50   Zhiqiang Shen and Marios Savvides. Meal v2: Boosting vanilla resnet-50 to 80%+ top-1 accuracy on imagenet without tricks. *arXiv preprint arXiv:2009.08453*, 2020.

51   Jia Deng, Wei Dong, Richard Socher, Li-Jia Li, Kai Li, and Li Fei-Fei. Imagenet: A large-scale hierarchical image database. In *2009 IEEE conference on computer vision and pattern recognition*, pages 248–255. Ieee, 2009.

52   Kaiming He, Xiangyu Zhang, Shaoqing Ren, and Jian Sun. Delving deep into rectifiers: Surpassing human-level performance on imagenet classification. In *Proceedings of the IEEE international conference on computer vision*, pages 1026–1034, 2015.